

Epitaxial crystalline film with pseudo-tenfold symmetry formed by Au-deposition on a decagonal $\text{Al}_{72}\text{Ni}_{12}\text{Co}_{16}$ quasicrystal

M. Shimoda, T. J. Sato, and A. P. Tsai

National Research Institute for Metals, 1-2-1, Sengen, Tsukuba-shi, Ibaraki, 305-0047, Japan

J. Q. Guo

CREST, Japan Science and Technology Corporation, Kawaguchi, Saitama, 332-0012, Japan

(Received 5 July 2000)

We have succeeded in growing an epitaxial film on a quasicrystal. Au-depositions on a quasiperiodic surface of a decagonal Al-Ni-Co quasicrystal gave rise to an epitaxial film with a tenfold symmetry, i.e., a layer of multiply twinned AuAl_2 crystals with (110)-oriented surfaces and azimuthal orientations corresponding to the tenfold symmetry of the substrate.

Since thermodynamically stable quasicrystals were found in an Al-Li-Cu alloy,^{1,2} the quasicrystalline phase has been recognized as one of the stable solid phases. While crystals, another stable solid phase, possess both the orientational and the translational long-range orders, quasicrystals preserve only the orientational long-range order. The properties of quasicrystalline alloys are unique. The electric conductivity is extraordinarily low in comparison with metals. Besides, it increases with temperature and decreases when the structural perfection improved. The heat conductivity is unusually low. Moreover, the hardness is very large. These properties originate in significantly modified electronic structures, such as formation of a pseudogap near the Fermi level, due to the quasiperiodic order.³ Until now, all quasicrystals were discovered in alloys. If quasicrystalline states could form in various materials such as pure metals, oxides, and organic compounds, several novel phenomena or properties would be expected. Moreover, from the viewpoint of the basic research, it is interesting to create quasicrystals of simple substances, because theoretical investigations of quasicrystals could become easier. The fact that the quasicrystalline phase is obtained only in limited combinations of elements under certain conditions, however, suggests that the formation of a quasicrystal in a desired combination of elements is thermodynamically impossible.

In order to clear this hurdle, we adopted an artificial way, i.e., growing quasicrystalline films epitaxially on a quasicrystal surface (note that we stretch the meaning of "epitaxy" so as to describe the phenomenon that films grow on a quasiperiodic substrate with maintaining the directional order of the substrate). The decagonal Al-Ni-Co quasicrystal is a good candidate for this purpose, because, as a two-dimensional quasicrystal, it has well-defined quasiperiodic planes perpendicular to the tenfold axis.⁴ As already reported, the surface exposing the quasiperiodic plane (tenfold surface) has the same quasiperiodic structure as in the bulk.⁵⁻⁷ It is also found that the tenfold surface is thermodynamically stable,^{5,6} which is preferable for our purpose.

In the present paper, we report the results of an attempt to grow epitaxial quasicrystalline films of Au on the tenfold surface of Al-Ni-Co. Au is chosen because, under a certain circumstance, it has a tendency to form icosahedral and deca-

hedral clusters as small particles,⁸ which harmonizes with the tenfold symmetry of the quasicrystal surface.

The structure was investigated by reflection high-energy electron diffraction (RHEED) and x-ray photoelectron diffraction (XPD). The combination of these tools, one is sensitive to the long-range order (RHEED) and the other to the short-range order (XPD),⁹ is significantly powerful to study the surface which might lose the translational long-range order. The strong forward scattering peaks in XPD images give a direct measure of the direction of atomic bonding near the surface. The film thickness is estimated from x-ray photoelectron spectroscopy (XPS) spectra by comparing signal intensities such as Au 4*f*-Co 2*p* emissions.

A slice of sample with the quasiperiodic tenfold surface was cut from a large single-grained $\text{Al}_{72}\text{Ni}_{12}\text{Co}_{16}$ quasicrys-

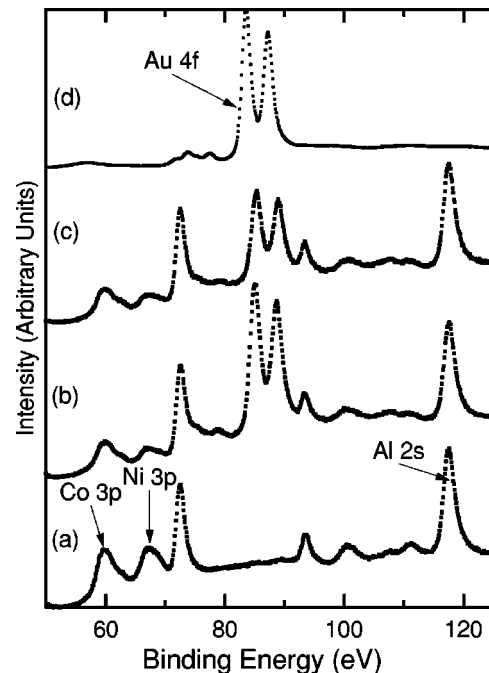


FIG. 1. XPS spectra from the tenfold surface of the decagonal $\text{Al}_{72}\text{Ni}_{12}\text{Co}_{16}$ quasicrystal, (a) after sputtering with Ar^+ ions, (b) after Au-depositions (~ 0.8 ML), (c) after annealing of the Au-deposited surface, and (d) XPS spectrum from a thick Au film.

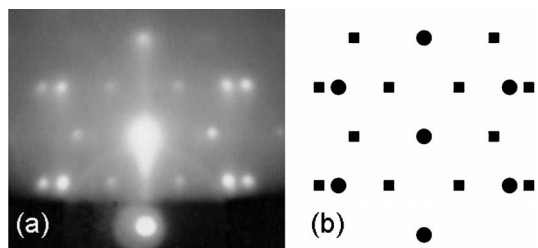


FIG. 2. (a) RHEED pattern from the tenfold surface of the decagonal $\text{Al}_{72}\text{Ni}_{12}\text{Co}_{16}$ quasicrystal after Au-depositions and the following annealing. The incident electron beams come along the A2D axis. (b) Schematic pattern of diffraction spots from an fcc crystal with (110)-oriented surface for [001] (filled circles) and $[\bar{1}12]$ (filled squares) incidence.

tal, which was prepared by the floating-zone method and confirmed to be of excellent quality.¹⁰ After mechanical polishing, the sample was transferred to the vacuum chamber (the base pressure $< 1 \times 10^{-8}$ Pa), where the stable quasiperiodic surface was prepared by several cycles of sputtering (30-min bombardment of 5-keV Ar^+ ions) and annealing (~ 700 K). The process of the surface treatments was moni-

tored by RHEED with 20-keV electrons at an emission current of 38 mA. XPS and XPD measurements were performed as described in Ref. 5.

Au depositions were performed at room temperature from a liquid-nitrogen-cooled evaporator with a tungsten basket. A quartz crystal oscillator was used as a thickness monitor. The deposition rate was 0.1–0.2 nm/min. The thickness of the overlayer is about 0.19 nm, which corresponds to 0.8 ML of Au in the closed-packed (111) structure. After the deposition, the sample was heated at a rate of 2 K/min. The pressure of the chamber was kept below 4×10^{-8} Pa during the evaporation and annealing.

It is known that, as a result of Ar^+ -ion bombardment, Al atoms are selectively sputtered and that the surface turns to a multiply twinned crystalline layer with a bcc-like structure.^{5,6} With annealing, however, the quasiperiodicity at the surface is restored. Therefore the quasiperiodic structure is stable even in the surface. Two types of clear RHEED patterns are observed from this surface for the incident electron beams along the A2P and A2D twofold axes (notations after Ref. 11) (shown in Fig. 1 of Ref. 5). Corresponding to the ten-

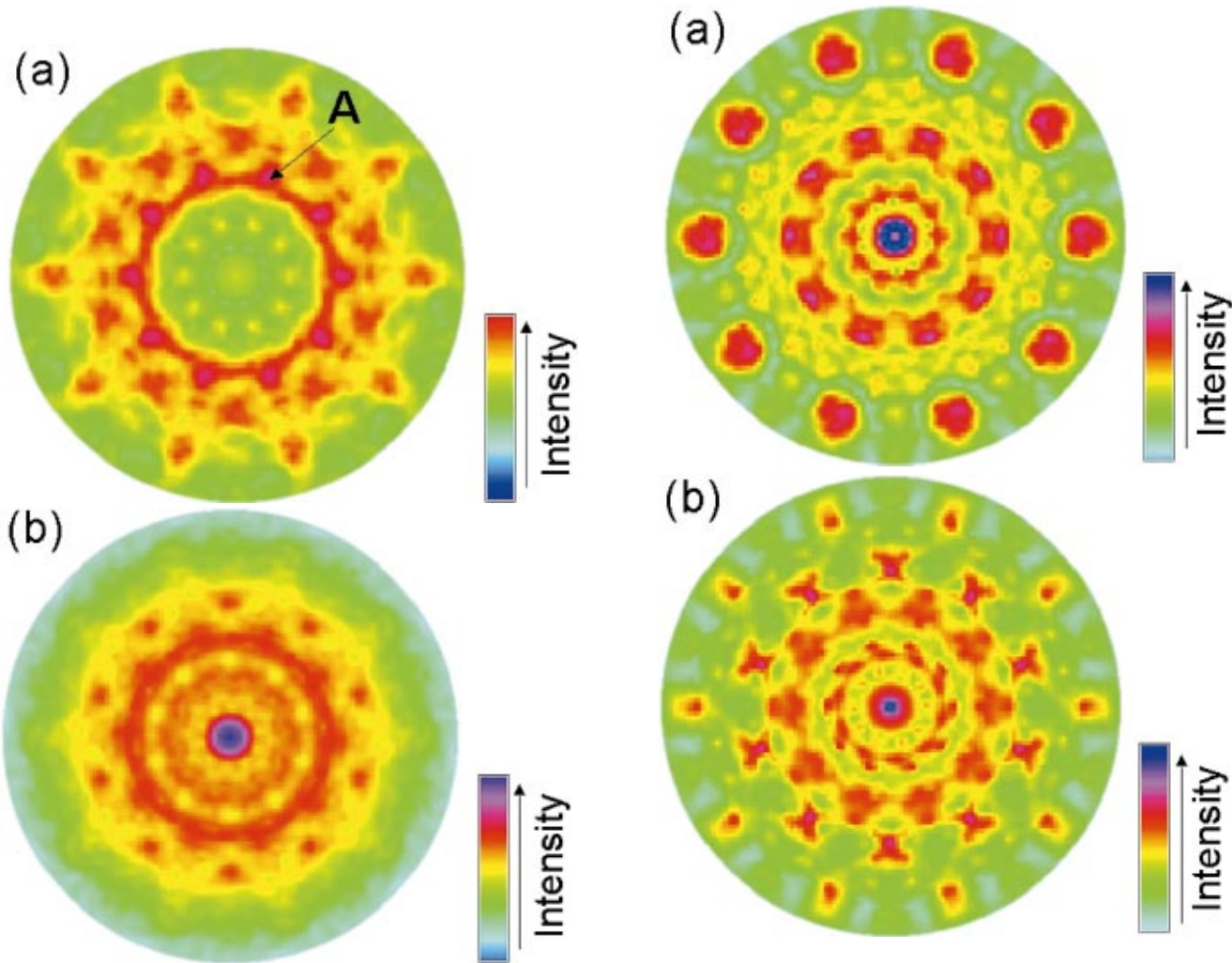


FIG. 3. (Color) Stereographic projections of XPD images of (a) Au 4*f* and (b) Al 2*s* photoemission from the tenfold surface of the decagonal $\text{Al}_{72}\text{Ni}_{12}\text{Co}_{16}$ quasicrystal after Au-depositions and the following annealing. These images are modified so as to enhance both the peak positions and the tenfold symmetry.

FIG. 5. (Color) Single scattering cluster simulations of XPD image for (a) Au 4*f* and (b) Al 2*s* photoemission from an epitaxial AuAl_2 layer. The effects of twinned crystals are introduced by superposing the images from single crystals with ten different orientations. According to the experimental images, the region from 0° to 70° in polar angle (θ) is presented.

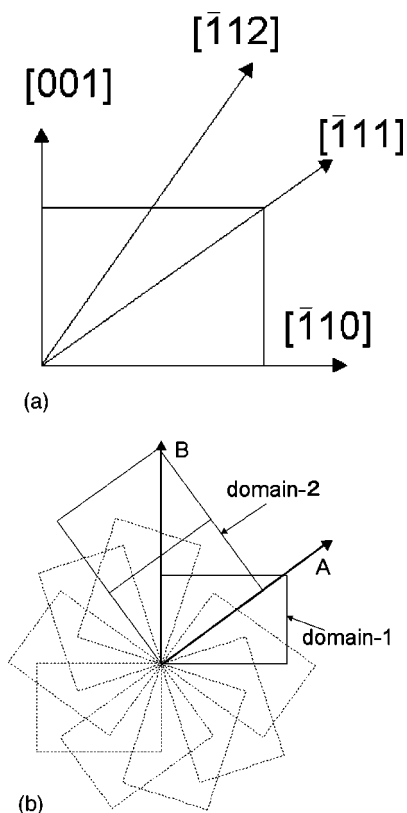


FIG. 4. Orientational relations among the twin-related fcc crystals with the (110)-oriented surface. Each rectangular represents the unit structure of an fcc (110) plane. The $[\bar{1}11]$ direction in the domain 1 (denoted by A) almost coincides with the $[\bar{1}10]$ direction in the domain 2, which is separated by 36° from the domain 1 for the rotation around the $[110]$ axis. Similarly, the direction B is regarded as $[001]$ in the domain 1 and, at the same time, as $[\bar{1}12]$ in the domain 2.

equivalent A2P and A2D axes, these patterns appear alternately every 18° for the rotation around the z axis (=the tenfold axis) of the quasicrystal. Accordingly, diffraction images of Al $2s$, Co $2p$ photoemission and Ni $L_3M_{45}M_{45}$ Auger electron from this surface show clear tenfold symmetric patterns. (also shown in Fig. 2 of Ref. 5).

Even after the Au depositions, the surface still shows the same RHEED patterns from the substrate except for a diffuse background, which is due to the Au overlayer. On the other hand, no prominent spots are observed in any XPD images within the range of the experiment, suggesting the Au atoms are deposited on the surface at random. As shown in Fig. 1, Au $4f$ photoemission spectrum for the as-deposited surface [Fig. 1(b)] exhibits a chemical shift of ~ 1.6 eV and a peak broadening of ~ 0.3 eV in comparison with the spectrum for a very thick Au film [Fig. 1(d)]. The shift and width of this spectrum are almost identical to the counterparts of the spectrum from the annealed surface [Fig. 1(c)], where Au-Al alloys are formed as discussed below. The intensities of Co $3p$ and Ni $3p$ photoemission decrease significantly after the deposition, while the intensity of Al $2s$ photoemission is almost unchanged. From these observations, we conclude that the deposition gives rise to a mixing of Au and Al and that a layer of randomly oriented Au-Al alloys are formed on the surface.

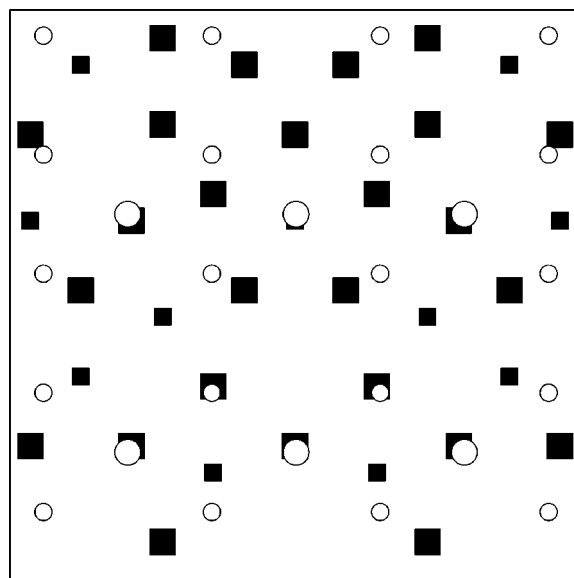


FIG. 6. A model for the interface between the overlayer and the substrate. Large and small circles represent Au and Al in the overlayer, respectively. Large and small solid squares represent Al and transition metals in the quasicrystalline plane of Al-Ni-Co. The coordinates of atoms in the quasicrystalline plane are given on the basis of the model in Ref. 18.

The effects of annealing are as follows. First, RHEED patterns from the substrate disappear at 350–400 K and are replaced with completely different patterns. The case for the incident electron beam along the A2D axis is shown in Fig. 2(a). Second, several strong peaks emerge in XPD images of Au $4f$ and Al $2s$ photoemission in a tenfold symmetric pattern [Figs. 3(a) and 3(b)]. Third, the relative intensity of Au $4f$ photoemission to other peaks decreases by half, whereas the peak position and width remain as before. No significant changes are observed for Co $3p$, Ni $3p$, and Al $2s$ photoemission spectra (Fig. 1).

RHEED patterns are interpreted as diffraction spots from an fcc crystal with (110)-oriented surface; the pattern in Fig. 2(a) is a superposition of patterns for the $[001]$ and $[\bar{1}12]$ incidence as shown in Fig. 2(b). Since the angle between $[001]$ and $[\bar{1}12]$ is very close to 36° (35.26° , to be exact), this superposition could be generated by twin-related fcc crystals with the (110)-oriented surface and different azimuthal orientations corresponding to the ten-equivalent A2D axes (see Fig. 4). Similarly, the pattern observed along the A2P axis is decomposed into patterns for the $[\bar{1}11]$ and $[\bar{1}10]$ incidence. The lattice constant estimated from these patterns is about 0.6 nm, which is much larger than 0.408 nm for the fcc Au crystal and very close to 0.5998 nm for the CaF_2 -type AuAl_2 .^{12,13}

These facts indicate the formation of an epitaxial layer of AuAl_2 . XPD images are perfectly explained with this structure as shown in Fig. 5, where the results of single scattering cluster simulations⁹ are presented. The cluster we used includes 14 emitters placed on the first five layers from the (110) surface.

It is clear that the positions of major peaks, i.e., the directions for the strong forward scattering, are well reproduced. The reproducibility of the relative intensity among the peaks

is not good because the effects of the multiple scattering and the contribution from the bulk are ignored. More straightforward interpretations are possible for the strong peaks. For example, the peaks found on the concentric circle at $\theta \sim 35^\circ$ in Fig. 3(a) (denoted by A) are assigned to, as one of the origins, the forward scattering along the $[111]$; a direction where atoms are densely chained. The decrease in the intensity of Au $4f$ photoemission in the XPS spectra is due to the penetration of Au atoms into deeper sites as a result of alloying.

As for the interface between the overlayer and the substrate, we have no information except for the orientational relations. However, the mismatch between the pentagonal units in the quasiperiodic plane¹⁴⁻¹⁸ and the lattice formed by Al and Au atoms in the (110) plane of AuAl_2 could be locally small, as illustrated in Fig. 6. This reminds us of the case for the sputtered surface of Al-Ni-Co,^{5,6} where the formation of CsCl-type AlCo (or AlNi) with a lattice constant of 0.286 nm (0.289 nm) are suggested. In AuAl_2 crystal, Al atoms form a cubic lattice with a lattice constant of ~ 0.3 nm.

Therefore we conclude that the same mechanism acts for the formation of the (110)-oriented surface in both the sputtered surface and the Au-deposited surface. Although we were unable to obtain the desired quasicrystalline layer of Au, our results show that the heteroepitaxy on the quasicrystal surface is possible. It should be pointed out that the quasicrystalline substrate played a critical role in creating a multiply twinned layer with tenfold symmetry. This occurs only when quasicrystalline substrate is used. Instead of Au, elements immisible to elements in the substrate could be a good candidate for quasicrystalline films.

In summary, we performed Au-depositions on the surface of the decagonal $\text{Al}_{72}\text{Ni}_{12}\text{Co}_{16}$ quasicrystal with an aim of growing quasicrystalline Au films. At room temperature, Au-Al alloys are formed without any orientational order. As a result of annealing, the surface turned to an epitaxial layer of multiply twinned AuAl_2 crystals.

This work was partly supported by CREST, Japan Science and Technology Corporation.

¹B. Dubost, J.M. Lang, M. Tanaka, P. Sainfort, and M. Audier, *Nature (London)* **324**, 48 (1986).

²A.-P. Tsai, A. Inoue, and T. Masumoto, *Jpn. J. Appl. Phys., Part 2* **26**, L1505 (1987).

³C. Janot, *Phys. Rev. B* **53**, 181 (1996).

⁴A.-P. Tsai, A. Inoue, and T. Masumoto, *Mater. Trans., JIM* **30**, 463 (1989).

⁵M. Shimoda, J.Q. Guo, T.J. Sato, and A.-P. Tsai, *Surf. Sci.* **454-456**, 11 (2000).

⁶M. Zurkirch, B. Bolliger, M. Erbudak, and A.R. Kortan, *Phys. Rev. B* **58**, 14 113 (1998).

⁷B. Bolliger, M. Erbudak, M. Hochstrasser, A.R. Kortan, and M. Zurkirch, *Phys. Rev. B* **54**, R15 598 (1996).

⁸S. Ino, *J. Phys. Soc. Jpn.* **21**, 346 (1966).

⁹C.S. Fadley, *Synchrotron Radiation Research, Advances in Surface Science*, edited by R.Z. Bachrach (Plenum, New York, 1989).

¹⁰T.J. Sato, T. Hirano, and A.-P. Tsai, *J. Cryst. Growth* **191**, 545 (1998).

¹¹Y. Qin, R. Wang, Q. Wang, Y. Zhang, and C. Pan, *Philos. Mag. Lett.* **71**, 83 (1995).

¹²C.D. West and A.W. Peterson, *Z. Kristallogr.* **A88**, 93 (1934).

¹³M.E. Straumanis and K.S. Chopra, *Z. Phys. Chem. (Frankfurt)* **42**, 344 (1964).

¹⁴A. Yamamoto, K. Kato, T. Shibuya, and S. Takeuchi, *Phys. Rev. Lett.* **65**, 1603 (1990).

¹⁵S.E. Burkov, *Phys. Rev. Lett.* **67**, 614 (1991).

¹⁶K. Saitoh, K. Tsuda, M. Tanaka, K. Kaneko, and A.-P. Tsai, *Jpn. J. Appl. Phys., Part 2* **36**, L1400 (1997).

¹⁷Y. Yan, S.J. Pennycook, and A.-P. Tsai, *Phys. Rev. Lett.* **81**, 5145 (1998).

¹⁸E. Abe, K. Saitoh, H. Takakura, A.-P. Tsai, P.J. Steinhardt, and H.-G. Jeong, *Phys. Rev. Lett.* **84**, 4609 (2000).